GYNECOLOGY

# Impact of polypropylene prolapse mesh on vaginal smooth muscle in rhesus macaque



Rebecca M. Shaffer, MD[1]; Rui Liang, MD[1]; Katrina Knight, PhD; Charelle M. Carter-Brooks, MD; Steven Abramowitch, PhD; Pamela A. Moalli, MD, PhD

**BACKGROUND:** The use of polypropylene prolapse mesh to treat pelvic organ prolapse has been limited by mesh-related complications. Gynemesh PS mesh, implanted via sacrocolpopexy in rhesus macaques, had a negative impact on the vagina with thinning of vaginal muscularis and decreased vaginal smooth muscle contractility. The negative effect was attenuated when a bioscaffold derived from urinary bladder extracellular matrix was used as a composite with Gynemesh PS.

**OBJECTIVE:** The objective of the study was to further elucidate the impact of Gynemesh PS polypropylene mesh and MatriStem extracellular matrix bioscaffolds on the vaginal smooth muscle in terms of micromorphology of vaginal smooth muscle (muscle bundles and individual myocytes), innervation, and nerve-mediated contractile function following their implantations in a rhesus macaque model via sacrocolpopexy.

**STUDY DESIGN:** Thirty-two middle-aged rhesus macaques were randomized to undergo either a sham surgery (sham, n = 8), or the implantation of Gynemesh PS alone (n = 8) vs composite mesh comprised of Gynemesh PS plus 2-ply MatriStem (n = 8) vs 6-ply MatriStem alone (n = 8) via sacrocolpopexy. The graft-vagina complexes were harvested 3 months later. Histomorphometrics of smooth muscle bundles and myocytes were performed by immunofluorescent labeling of alpha smooth muscle actin, caveolin-3 (membrane protein), and cell nuclei followed by confocal imaging. The cross-sectional diameters of smooth muscle bundles and individual myocytes were quantified using images randomly taken in at least 5 areas of each section of sample. Contractile proteins alpha smooth muscle actin and smoothelin were quantified by Western immunoblotting. Nerve density was measured by immunohistochemical labeling of a pan-neuron marker, PGP9.5. Nerve-mediated smooth muscle contractility was quantified using electrical field stimulation. One-way analysis of variance and appropriate post hoc tests were used for statistical comparisons.

**RESULTS:** Compared with sham, the implantation of Gynemesh PS alone resulted in a disorganized smooth muscle morphology with the number of small muscle bundles (cross-sectional diameter less than 20 $\mu$m) increased 67% ($P = .004$) and the myocyte diameter decreased 22% ($P < .001$). Levels of contractile proteins were all decreased vs sham with alpha smooth muscle actin decreased by 68% ($P = .009$), low-molecular-weight smoothelin by 51% ($P = .014$), and high-molecular-weight smoothelin by 40% ($P = .015$). Nerve density was decreased by 48% ($P = .03$ vs sham) paralleled by a 63% decrease of nerve-mediated contractility ($P = .02$). Following the implantation of composite mesh, the results of measurements were similar to sham (all $P > .05$), with a 39% increase in the myocyte diameter ($P < .001$) and a 2-fold increase in the level of alpha smooth muscle actin relative to Gynemesh ($P = .045$). Following the implantation of MatriStem alone, the number of small muscle bundles were increased 54% vs sham ($P = .002$), while the other parameters were not significantly different from sham (all $P > .05$).

**CONCLUSION:** The implantation of Gynemesh PS had a negative impact on the structural and functional integrity of vaginal smooth muscle evidenced by atrophic macro- and microscopic muscle morphology, decreased innervation, and impaired contractile property, consistent with a maladaptive remodeling response. The extracellular matrix bioscaffold (MatriStem), when used with Gynemesh PS as a composite (2 ply), attenuated the negative impact of Gynemesh PS; when used alone (6 ply), it induced adaptive remodeling as evidenced by an increased fraction of small smooth muscle bundles with normal contractility.

**Key words:** contractility, innervation, prolapse, micromorphology, smooth muscle, synthetic mesh, rhesus macaque

Symptomatic pelvic organ prolapse is a common debilitating gynecological condition, affecting 6−31% of the general population, with an estimated 12.6% lifetime risk for women of undergoing a surgical repair by age 80 years.[1−6] While a woman's own tissues are often used to restore support to the pelvic organs, large multicenter trials show that 40% of these surgeries fail by 2 years,[7,8] and the rate increases to 70% at 5 years.[9]

Polypropylene meshes are frequently used to overcome the limitations of native tissue repairs. Unfortunately, meshes have been associated with increased complications,[10] most commonly mesh exposure through the vaginal epithelium and/or pain, despite improved anatomical outcomes.[11,12] The impact of polypropylene mesh on the vagina and the mechanism of complications are not completely understood.

In a primate sacrocolpopexy model, Gynemesh PS (Gynemesh), a commonly used prototype of urogynecological mesh (Ethicon, Somerville, NJ), induced thinning of the vagina with the greatest impact on the thickness of the vaginal smooth muscle layer (muscularis) and vaginal contractility.[13,14] Such degenerative changes likely negatively affect the maintenance of vaginal tone and future sexual function, thus having important implications for a women's quality of life. To overcome these mesh-induced degenerative changes in the vaginal smooth muscle, a better understanding of the pathogenesis is necessary.

**Cite this article as:** Shaffer RM, Liang R, Knight K, et al. Impact of polypropylene prolapse mesh on vaginal smooth muscle in rhesus macaque. Am J Obstet Gynecol 2019;221:330.e1-9.

0002-9378/$36.00

https://doi.org/10.1016/j.ajog.2019.05.008

Click Supplemental Materials under article title in Contents at ajog.org

## AJOG at a Glance

### What is the purpose of this study?

Polypropylene prolapse mesh has a negative impact on vaginal smooth muscle structure and function, which is undesirable. Here we aim to define the mechanism by which polypropylene mesh exerts its negative effects and further explore whether the use of an extracellular matrix bioscaffold can modify this response.

### Key findings

Implantation of a polypropylene mesh (Gynemesh PS) induced a maladaptive remodeling response in vaginal smooth muscle evidenced by atrophic macro- and microscopic muscle morphology, decreased innervation, and decreased contractility. An extracellular matrix bioscaffold, when used in conjunction with polypropylene mesh as a composite (2-ply), attenuated the negative impact. When used alone, the bioscaffold (6-ply) induced tissue remodeling as evidenced by an increased proportion of small smooth muscle bundles but with normal myocyte size and normal contractility.

### What does this add to what is known?

This study provides critical insight into mechanisms by which Gynemesh PS exerts a negative impact on vaginal smooth muscle structure and function and the modification of that response via application of an extracellular matrix bioscaffold.

As one of the stiffest prolapse meshes available on the market with a stiffness measured at 0.29 ± 0.02 N/mm,[15,16] the implantation of Gynemesh on the vagina is likely to induce stress shielding, a phenomenon occurring when a stiffer material (mesh) shields the softer material (vagina) from forces it normally sustains. Resultantly, the less stiff material undergoes a maladaptive remodeling response characterized by degeneration and atrophy, often resulting in functional impairment.[17−20]

We hypothesize that Gynemesh induces a maladaptive remodeling response in the vaginal smooth muscle through stress shielding, resulting in thinning of muscle layer with atrophy of muscle bundles and myocytes.

In addition, we have shown that a non-cross-linked extracellular matrix (ECM) bioscaffold, MatriStem (ACELL, Columbia, MD), when used in conjunction with Gynemesh as a composite mesh, attenuated the negative impact of Gynemesh on the vagina. ECM bioscaffolds have been shown to promote tissue reconstructive remodeling and facilitate tissue regeneration through immune modulation and progenitor cell recruitment.[21,22] Thus, we further hypothesize that the microstructure of vaginal smooth muscle will be improved by the ECM component in the composite mesh.

In this study, we aimed to test our hypotheses by characterizing the microstructure and contractile components of vaginal smooth muscle following the implantation of Gynemesh and the composite mesh with a 2-ply MatriStem via sacrocolpopexy in a rhesus macaque model. To determine the independent impact of the ECM bioscaffold on the vagina, we also implanted a 6-ply MatriStem alone.

Our rationale for using a 6-ply alone vs a 2-ply in the composite was to maintain the initial stiffness of each implant to be similar to that of Gynemesh. Experimental measurements included cross-sectional diameters and size distributions of muscle bundles and myocytes and expression of smooth muscle contractile proteins (alpha smooth muscle actin (αSMA) and smoothelin). Because innervation is critical for maintaining normal smooth muscle morphology and function,[23] we also characterized the nerve density (PGP9.5; a pan-neuron marker) with a test of nerve-mediated smooth muscle contractility.

## Materials and Methods

The Institutional Animal Care and Use Committee at the University of Pittsburgh authorized the use of nonhuman primates for this study under Institutional Animal Care and Use Committee number 1008675.

### Surgery

Tissues samples tested in this study were acquired as described.[14,24] Briefly, 32 middle-aged parous rhesus macaques (*Macaca mulatta*) underwent procedures of sacrocolpopexy after hysterectomy. Animals were randomized to undergo either sham surgery (sham, n = 8) or implantation of Gynemesh PS (Gynemesh, n = 8), a composite mesh comprised of Gynemesh plus 2-ply MatriStem (composite, n = 8) or a 6-ply MatriStem alone (MatriStem, n = 8). All animals had regular menstrual cycles and were noted to have minimal prolapse (no prolapse past the hymen) on standardized preoperative evaluation.

For the implantation of grafts, individual 3 × 10 $cm^2$ straps of Gynemesh, composite mesh, or 6-ply MatriStem were sutured to the anterior and posterior walls of the vagina using 3-0 polydioxanone suture (Ethicon) and then fixed to the longitudinal ligament of the sacrum at S1−S2 using 2 individual delayed absorbable sutures. In the sham surgeries, the same dissections were performed but no mesh was implanted.

### Sample preparation

At 3 months following implantation, the graft-vagina complexes (GVCs) were removed en bloc and the anterior portion of the GVCs were processed for the purposes of morphological, biochemical and contractile experiments. For histomorphological testing, full-thickness tissue biopsies were obtained from the anterior grafted vaginal wall, approximately 2 cm from the apex and 1 × 0.5 $cm^2$ in size, fixed in 4% paraformaldehyde, and embedded in optimum cooling temperature medium (Tissue-Tek; Miles Laboratories Inc, Elkhart, IN).

**TABLE 1**
**Demographics of nonhuman primates in the study**

| Groups | Age (y) | Gravidity | Parity | Weight (kg) |
|---|---|---|---|---|
| Sham (n = 8) | 11 (10, 15) | 5 (2.75, 6) | 2 (1.75, 4.5) | 7.1 ± 1.3 |
| Gynemesh PS (n = 8) | 13 (11.5, 14) | 5 (4, 5.75) | 3.5 (2, 4) | 8.0 ± 1.7 |
| Composite (n = 8) | 8 (7, 10.25) | 3 (1.75, 5) | 2 (1.75, 4.25) | 7.8 ± 1.9 |
| MatriStem (n = 8) | 13.5 (12.25, 14) | 4 (3.75, 5) | 3.5 (3, 4.25) | 8.5 ± 1.4 |
| *P* value[a] | .05 | .356 | .777 | .597 |

Results are expressed as mean ± SD for weight or median (first quartile, third quartile) for age, gravidity, and parity.

[a] Overall comparison of *P* value among the groups.

*Shaffer et al. Impact of mesh implantation on vaginal smooth muscle. Am J Obstet Gynecol 2019.*

For biochemical analysis, the tissue was snap frozen in liquid nitrogen, pulverized, and stored at −80°C. For contractility testing, circumferential vaginal strips of GVCs measuring approximately 2 × 7 $mm^2$ were dissected and tested within 30 minutes of tissue harvest.

## Immunofluorescence for the microstructures of vaginal smooth muscle

The tissue blocks were cut into 7 μm and oriented such that the tissue was cut 90° to the longitudinal axis of vagina. Caveolin-3 was used to label the cell membrane of individual myocytes.[25,26] αSMA was labeled to delineate the cytoskeleton of muscle cells and boundary of muscle bundles.

Tissue sections were incubated with a mouse monoclonal anti-αSMA (Sigma, St Louis, MO) at 1:150 for 2 hours at room temperature followed by a goat polyclonal antibody caveolin-3 (Santa Cruz Biotechnology, Dallas, TX) at 1:50 overnight at 4°C. Secondary antibodies were then applied including Texas Red conjugated donkey antimouse (Vector, Burlingame, CA) at 1:300, and fluorescein isothiocyanate conjugated bovine antigoat (Jackson ImmunoResearch, West Grove, PA) at 1:300. 4′, 6-Diamidino-2-phenylindole was included in the mounting medium (Vectashield mounting medium with 4′, 6-diamidino-2-phenylindole; Vector) for labeling of nuclei.

For analysis, 5 randomly selected fields per section were analyzed using a 90i Nikon light-fluorescence microscope (Nikon Instruments, Melville, NY) using a ×20 objective for smooth muscle bundles or a Nikon A1 confocal microscope using a ×60 objective for individual myocytes. Images were analyzed using NIS-Elements AR3.2 software (Nikon). Smooth muscle bundles and individual myocytes were outlined circumferentially and the minimum cross-sectional diameters were extrapolated using the software measured as miniferets.

## Immunohistochemistry for the innervation of vaginal smooth muscle

PGP9.5, a general marker for neuronal cell bodies and axons, was labeled. The tissue sections were incubated with a mouse monoclonal antibody for PGP9.5 (Abcam, Cambridge, MA) at 1:150 overnight at 4°C. Horseradish peroxidase conjugated donkey antimouse antibody (Vector) was then applied for 1 hour at room temperature. The color was developed using diaminobenzidine substrate kit (Abcam) followed by a counterstain using hematoxylin (Sigma). Brown color denoted positive labeling. Nerve density was reported as the percentage of PGP9.5-positive area relative to the measured muscle area.

## Western blot for contractile proteins

Following tissue extraction using a high-salt buffer (pH 7.5) as previously described,[27] total protein concentration was determined (DC protein assay; Bio-Rad, Hercules, CA). Primary antibodies included αSMA at 1:500 (SAB2500963, goat polyclonal; Sigma), and smoothelin at 1:500 (R4A, mouse monoclonal; Invitrogen, Rockford, IL).

Signal intensity of bands was visualized on ChemiDoc touch imaging system (Bio-Rad) and quantitated via Image Lab (version 5.2.1; Bio-Rad). The blotted membranes were stained with Coomassie Blue and the protein bands were quantified as loading controls for each well. Protein amounts were expressed as arbitrary units, relative to the loading control and an internal positive control (protein extract from a human prolapsed vagina) that was loaded in duplicate on each gel.

## Contractility testing

An electrical field stimulation (EFS) test was performed as described.[28] Contractile responses are reported as proportions of maximal contractility responses induced chemically using 120 mM potassium chloride that were reported in our previous study.[14] Historical data for sham and Gynemesh[29] were reviewed for the comparisons with the data obtained for the composite mesh and MatriStem.

## Statistical analysis

Sample size was determined using previous published data (smooth muscle thickness and contractility) for sham and Gynemesh PS,[13,24] in which at least 8 animals were needed in each group to achieve significance with α error of 0.05 and power of 0.80. Statistical comparisons were made using SPSS 18.0 (SPSS Inc, Chicago, IL).

FIGURE 1
**Morphology and sizes of smooth muscle bundles in vagina**

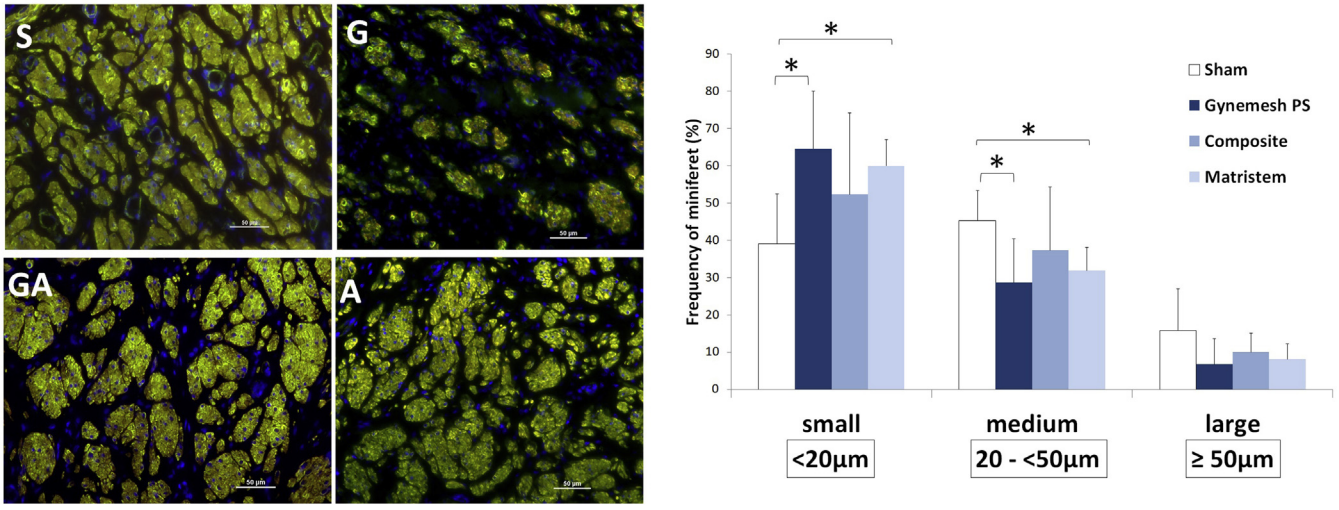


Morphology and sizes (diameter as measured by miniferet) of smooth muscle bundles in the vagina at 3 months following the implantation of Gynemesh PS, composite mesh, and 6-ply MatriStem. *Green* represents immunofluorescent labeling of caveolin-3; *red* represents immunofluorescent labeling of $\alpha$ smooth muscle actin; *blue* represents nuclei. Scale bar = 50 $\mu$m. Asterisk indicates statistical difference with $P < .01$.

*A*, 6-ply MatriStem; *G*, Gynemesh PS; *GA*, Gynemesh PS plus 2-ply MatriStem; *S*, sham.

*Shaffer et al. Impact of mesh implantation on vaginal smooth muscle. Am J Obstet Gynecol 2019.*

Because all data followed a normal distribution, 1-way analysis of variance with a Tukey post hoc procedure comparing between groups and a Dunnett procedure comparing experimental groups with sham was performed. Because the muscle bundles were categorized by size and represented by percentages, the data were also analyzed using Kruskal-Wallis tests with Mann-Whitney tests (adjusted for multiple comparisons) to compare between groups. Significance was set at $P < .05$.

## Results

Demographic data showed no overall differences in age, gravidity, parity, or weight among the groups (Table 1). Because animals in the composite group were younger than those in the sham ($P = .028$), multivariable regression modeling was performed, which showed that age did not have an impact on any of the experimental outcomes ($P > .15$).

### Histomorphometrics of vaginal smooth muscle bundles

Vaginal smooth muscle bundles were clearly demarcated. Following the implantation of Gynemesh, muscle bundles appeared small and scattered, whereas bundles in the sham group appeared larger and more organized (Figure 1). The average size of muscle bundles was not significantly different between sham and Gynemesh ($P = .06$, Table 2). However, when bundle sizes were grouped into small- (<20 $\mu$m), medium- (20−50 $\mu$m), and large (>50 $\mu$m)-sized bundles, small bundles in Gynemesh were increased by 67% (65% ± 15% in Gynemesh vs 39% ± 13% in sham, $P = .028$) with a proportionally decreased number of medium bundles (29% ± 12% in Gynemesh vs 45% ± 8% in sham, $P = .028$) and no difference in the number of large bundles (6% ± 7% in Gynemesh vs 16% ± 11% in sham, $P = .23$).

With the composite mesh, muscle bundles appeared more organized when compared with Gynemesh (Figure 1). The numbers of small (52% ± 22%), medium (37% ± 17%), and large (10% ± 5%) bundles were not significantly different from sham ($P = .16$, $P = .18$, and $P = .44$, respectively) or Gynemesh ($P = .61$, $P = .61$, and $P = .28$, respectively). The average diameter of muscle bundles in the composite mesh was between the values of sham and Gynemesh (composite vs sham, $P = .33$; composite vs Gynemesh, $P = .41$, respectively, Table 2).

With the 6-ply MatriStem alone, the muscle bundles appeared smaller but were well organized, similar to sham (Figure 1). The number of small bundles (60% ± 7%) was increased by 54% (MatriStem vs sham, $P = .033$) with a parallel decrease in the medium (32% ± 6%, MatriStem vs sham, $P = .039$) and large (8% ± 4%, Matristem vs sham, $P = .13$) bundles relative to sham. The average diameter of muscle bundles in the MatriStem was 26% lower than the sham (MatriStem vs sham, $P = .018$, Table 2).

### Histomorphometrics of vaginal smooth muscle myocytes

Following Gynemesh implantation, myocytes appeared irregular and flattened as opposed to cuboidal or round-like myocytes present in sham (Figure 2). The average size of individual myocytes, represented by minimal

**TABLE 2**
**Functional and morphometric analysis of the vaginal smooth muscle after the implantation of Gynemesh PS (n = 8), composite mesh (n = 8), and 6-ply MatriStem (n = 8) as compared with sham (n = 8)**

| | Morphometrics | | Innervation | Contractility |
|---|---|---|---|---|
| Variables | Bundle size in average (μm) | Myocyte size in average (μm) | Nerve density (ratio) | EFS (g/g) |
| Sham | 30.5 ± 8.0 | 3.6 ± 0.3 | 0.048 ± 0.016 | 0.48 ± 0.28[a] |
| Gynemesh PS | 22.4 ± 7.2 | 2.8 ± 0.2[b] | 0.024 ± 0.009[b] | 0.18 ± 0.16[a,b] |
| Composite | 26.1 ± 9.5 | 3.9 ± 0.6 | 0.054 ± 0.027 | 0.41 ± 0.24 |
| MatriStem | 22.5 ± 2.8[b] | 3.4 ± 0.2 | 0.045 ± 0.011 | 0.47 ± 0.25 |
| *P* value[c] | .117 | < .001 | .114 | .281 |

Results are expressed as mean ± standard deviation. EFS: electrical field stimulation.

[a] historical data.[29]; [b] $P < .05$ when compared with sham; [c] *P* values of overall comparisons among groups.

*Shaffer et al. Impact of mesh implantation on vaginal smooth muscle. Am J Obstet Gynecol 2019.*

cross-sectional diameter, was 22% smaller as compared with sham (2.8 ± 0.2 μm in Gynemesh vs 3.6 ± 0.3 μm in sham, $P < .001$, Table 2).

The distribution histograms of the diameter of individual myocytes showed that the peak value of sham centered at 3−4 μm, whereas the peak value of Gynemesh shifted left and centered at 3 μm. There were significantly more myocytes with diameters smaller than 3 μm and fewer myocytes with diameters larger than 5 μm in the Gynemesh as compared with sham (all $P < .01$, Figure 2).

With the composite mesh, the myocytes showed a typical round contour similar to sham (Figure 2). The average cell size was measured at 3.9 ± 0.6 μm, which was 39% larger than that for Gynemesh (composite vs Gynemesh, $P < .001$) and similar to that of sham (composite vs sham, $P = .2$, Table 2). The distribution histogram of myocyte diameters exhibited a pattern similar to sham.

With MatriStem alone, the myocytes appeared round with a similar appearance to that of sham (Figure 2). The average cell size was 3.4 ± 0.2 μm, which was 21% larger than that for the Gynemesh (MatriStem vs Gynemesh, $P < .001$) and similar to sham (MatriStem vs sham, $P = .28$, Table 2). The distribution histogram of myocyte diameters showed a pattern similar to sham (Figure 2).

## Vaginal contractile proteins

A single band (~42 kDa) was detected for αSMA and 3 bands (~130, 70, and 73 kDa) for smoothelin (Figure 3). Smoothelin is a marker of highly differentiated contractile smooth muscle cells with a long isoform typically expressed in vessels and a short isoform expressed in visceral muscle.[30] Here we identified the long isoform at approximately 130 kDa (smoothelin high molecular weight [HMW]) and the short isoform as a doublet at roughly 70 and 73 kDa (smoothelin low molecular weight [LMW]).

Following the Gynemesh implantation, both contractile proteins were reduced with αSMA decreased by 68%, smoothelin HMW by 40%, and smoothelin LMW by 51% relative to sham ($P = .009$, $P = .015$, $P = .014$, respectively). With the composite mesh, the level of αSMA was increased 2-fold over the Gynemesh (composite vs Gynemesh, $P = .045$) and was similar to sham (composite vs sham, $P = .48$). Smoothelin HMW and LMW were not statistically different from sham ($P = .21$ and $P = .24$, respectively) or Gynemesh ($P = .31$ and $P = .08$, respectively).

With the MatriStem alone, both contractile proteins were preserved with levels higher than Gynemesh (MatriStem vs Gynemesh: αSMA, $P = .003$, smoothelin HMW, $P = .038$, smoothelin LMW, $P = .041$) and close to sham (MatriStem vs Sham: αSMA, $P = .60$, smoothelin HMW, $P = .91$, smoothelin LMW, $P = .25$).

## Vaginal innervation

Overall nerve density was reduced by 48% following Gynemesh implantation as compared with sham (Gynemesh vs sham, $P = .033$, Table 2), consistent with prior report.[29] With the composite, the nerve density was restored to a level comparable with sham (composite vs sham, $P = .71$) but was not significantly different from Gynemesh (composite vs Gynemesh, $P = .08$). With MatriStem alone, the nerve density was not statistically different from the sham (MatriStem vs sham, $P = .74$) and was 47% higher than Gynemesh (MatriStem vs Gynemesh, $P = .019$).

## EFS contractility

The values of EFS contractility (Table 2), a measure of nerve-mediated smooth muscle contractility, paralleled our findings of nerve density. The contractility was significantly decreased by 63% in Gynemesh when compared with sham (Gynemesh vs sham, $P = .02$).[29] With the composite, the contractility was increased to a level close to sham (composite vs sham, $P = .55$) but not statistically different from Gynemesh (composite vs Gynemesh, $P = .05$). With the MatriStem alone, the contractility was similar to sham (MatriStem vs Sham, $P = .89$) and 62% higher than Gynemesh (MatriStem vs Gynemesh, $P = .02$).

FIGURE 2
**Morphology and size distribution of smooth muscle myocytes in vagina**

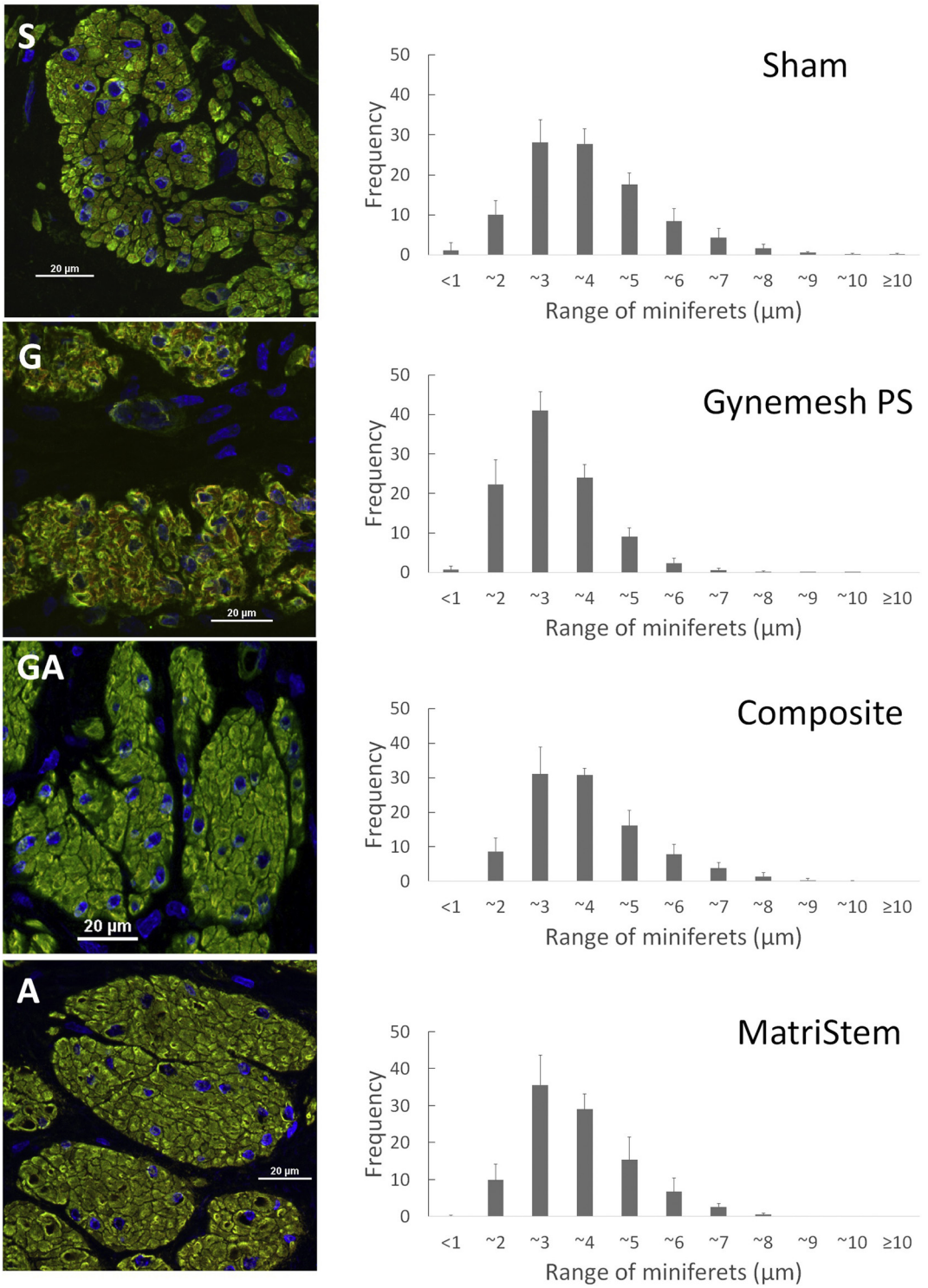


Morphology and size distribution (diameter as measured by miniferet) of smooth muscle myocytes in the vagina at 3 months following the implantation of Gynemesh PS, composite mesh, and 6-ply MatriStem. *Green* represents immunofluorescent labeling of caveolin-3; *red* represents immunofluorescent labeling of $\alpha$ smooth muscle actin; *blue* represents nuclei. Scale bar = 20 $\mu$m.

*A*, 6-ply MatriStem; *G*, Gynemesh PS; *GA*, Gynemesh PS plus 2-ply MatriStem; *S*, sham.

*Shaffer et al. Impact of mesh implantation on vaginal smooth muscle. Am J Obstet Gynecol 2019.*

FIGURE 3
**Semiquantification of contractile proteins**

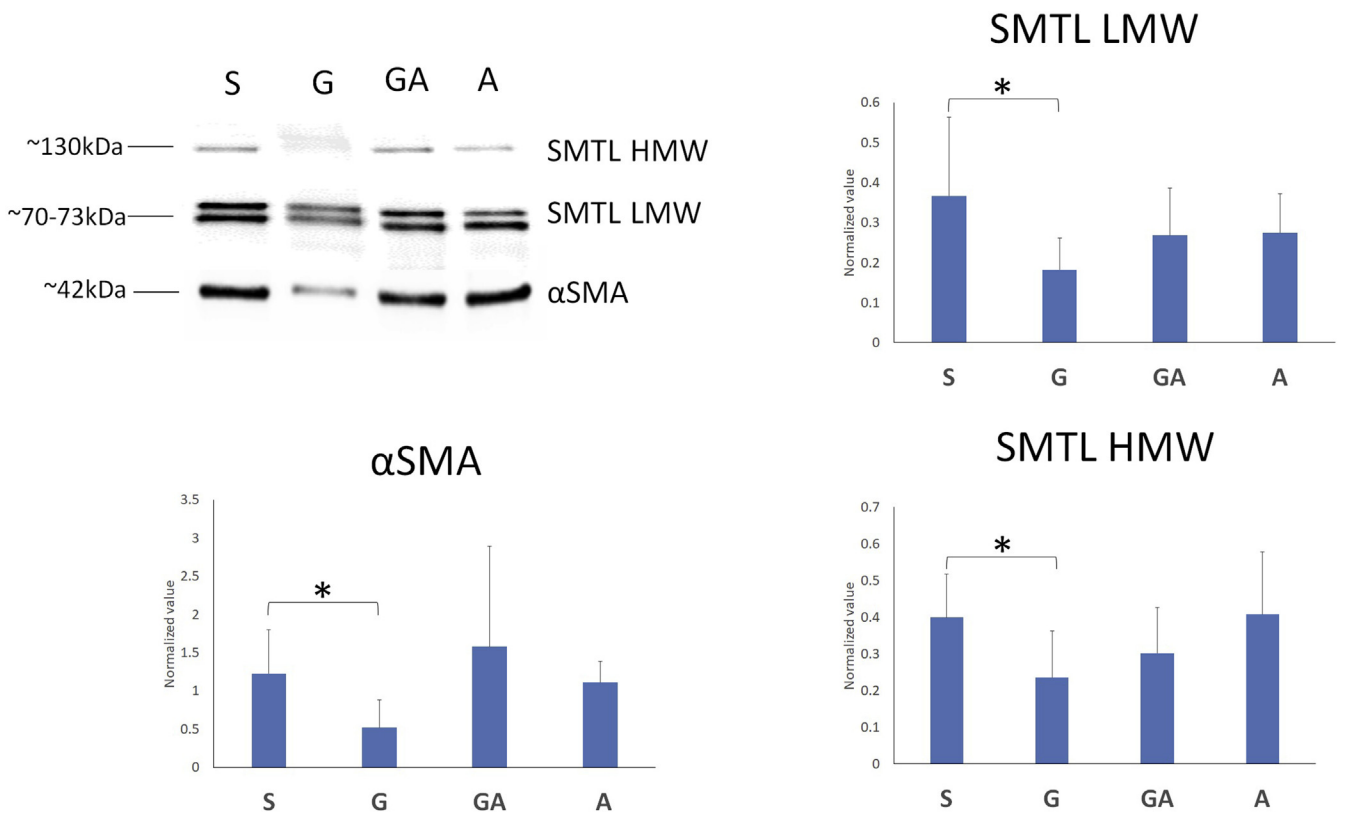


Semiquantification of contractile proteins: αSMA and SMTL in the vagina at 3 months following the implantation of Gynemesh PS, composite mesh, and 6-ply MatriStem. Asterisk indicates statistical difference with $P < .05$.

*A*, 6-ply MatriStem; *αSMA*, α smooth muscle actin; *G*, Gynemesh PS; *GA*, Gynemesh PS plus 2-ply MatriStem; *HMW*, high molecular weight; *LMW*, low molecular weight; *S*, sham; *SMTL*, smoothelin.

*Shaffer et al. Impact of mesh implantation on vaginal smooth muscle. Am J Obstet Gynecol 2019.*

## Comment

### Principal findings of this study

The findings of this study provide essential evidence towards exploring the mechanisms by which the implantation of Gynemesh and/or ECM bioscaffold has an impact on the vaginal smooth muscle structure and function in terms of micromorphology, contractile properties, and innervation. Gynemesh implantation resulted in an increase in smaller-sized smooth muscle bundles and myocytes with decreased expressions of contractile proteins and reduced nerve density, strongly supporting the hypothesis of smooth muscle atrophy following the mesh implantation.

The negative impact of Gynemesh was reversed, in part, by the 2-ply MatriStem in the composite mesh. When used alone, the 6-ply MatriStem may induce an adaptive response in the vaginal smooth muscle as evidenced by an increased fraction of small smooth muscle bundles with absence of altered myocyte size or contractile function.

### Interpretation of results and implications

In line with our previous observation that the loss of vaginal contractility following the implantation of Gynemesh was closely associated with the thinning of vaginal muscularis,[13,14,29] the findings of this study further suggest that the loss of contractile function is a cumulative result of atrophy, possibly induced by stress shielding. In virtually all other fields of biomaterials, stress shielding is known to induce a maladaptive remodeling response characterized by degeneration and atrophy, similar to what we have observed here.

As one of the stiffest prolapse meshes[15,16] on the market, Gynemesh has an unstable pore geometry, which further increases stiffness via pore collapse when the mesh is tensioned and loaded.[31,32] The ensuing differences in stiffness between the mesh and vagina become greater and increase the negative effect of stress shielding.

Because smooth muscle myocytes are highly sensitive to mechanical cues and undergo different plasticity changes when exposed to forces at variable degrees,[33,34] it is likely that the vaginal muscularis undergoes atrophy in response to the stress shielding brought by the implantation of Gynemesh. Notably, the stiffness of knitted

polypropylene mesh correlates positively to mesh weight and negatively to mesh porosity[15] (ie, less stiff mesh usually has lighter weight and higher porosity, properties being associated with an improved host response). Thus, to isolate the role of stiffness in the impact of mesh on the vaginal smooth muscle, it is necessary to control the other mesh properties (weight and porosity) in future investigations. While other factors such as mesh associated chronic inflammation may also play a role in the process of smooth muscle atrophy,[35–37] more studies are needed to fully elucidate the mechanisms of mesh-induced muscularis atrophy.

Given that women with prolapse already have compromised vaginal smooth muscle in terms of volume and bundle size,[38–41] further negative impact incurred with mesh implantation is undesirable. Corresponding to our previous findings that the composite mesh composed of Gynemesh and 2-ply MatriStem attenuated the degenerative changes of vagina induced by Gynemesh,[24] the current findings provided further evidence on the preventive role of MatriStem in the progression of smooth muscle atrophy, showing improvements in the size of myocytes and the levels of contractile proteins.

The ECM bioscaffold may function to attenuate the worsening effect of stress shielding of Gynemesh by stabilizing the mesh geometry, thereby physically preventing the mesh deformation (pore collapse and buckling). Furthermore, the bioscaffold may also play a role in dampening the proinflammatory responses in the local mesh area and facilitating the regeneration of smooth muscle.[42,43] Clinically, presurgical treatments that have positive effect on the structure of vaginal wall, such as topical application of estrogen, may be beneficial, while it is unclear whether such treatments also counteract the negative effect of mesh implantation.

Despite an initial stiffness similar to that of Gynemesh, the 6-ply MatriStem alone did not induce overall negative impact on the microstructure, innervation, and contractility of vaginal smooth muscle, which is in line with our previous findings.[24] Although the fraction of smaller smooth muscle bundles was increased, the mytocyte morphology and the content of contractile proteins were not altered. Together with the preservation of innervation and nerve-mediated contractility, these findings suggest that MatriStem induced an adaptive remodeling response. Any potential adverse effect of the initial high stiffness of 6-ply MatriStem may have been eliminated by rapid breakdown and remodeling of the bioscaffold during the process.

## Strengths and limitations

The main strengths of the study include the following: (1) a mechanistic study bringing new understanding of the impact of polypropylene mesh and/or ECM bioscaffold on the vaginal smooth muscle; and (2) the use of the rhesus macaque model, a robust animal model in pelvic organ prolapse research resembling human closely, allows control of variables.

One limitation of this study is that a relatively small number of animals was used. An increased sample size may have allowed us to see differences where they were not observed in this study such as the decrease of average size of muscle bundles in Gynemesh PS vs sham, and the improvement of nerve density and nerve-mediated contractility in the composite mesh relative to Gynemesh. Indeed, a post hoc power analysis showed that the current sample size was able to achieve 79% and 56% power to discern the differences of nerve density and contractility between composite mesh and Gynemesh respectively, suggesting that an increase in sample size will corroborate the findings of protective effect of 2-ply MatriStem in the composite mesh on vaginal muscularis. In addition, by using an animal model, we must extrapolate the results to applicability for human surgical interventions. Thus, more work is needed before the results can be directly translated to humans.

## Conclusions

The implantation of Gynemesh PS had a negative impact on the structural and functional integrity of vaginal smooth muscle, consistent with a maladaptive remodeling response. The ECM bioscaffold (MatriStem), when used with Gynemesh PS as a composite (2 ply), attenuated the negative impact of Gynemesh PS; when used alone (6 ply), induced an adaptive remodeling in the vaginal muscularis.

Future studies are warranted to elucidate the impact of mesh stiffness on the vaginal smooth muscle in animal models including the investigation of softer polymers better matched with the mechanical properties of the vagina. Such studies will inform future mesh designs for use in prolapse surgeries and improve outcomes of prolapse surgeries. ■

## Acknowledgment

We are grateful for the financial support from National Institutes of Health award R01 HD061811 and an institute cooperative research agreement with Acell Inc (Columbia, MD).

## References

1. Maclennan AH, Taylor AW, Wilson DH, Wilson D. The prevalence of pelvic floor disorders and their relationship to gender, age, parity and mode of delivery. BJOG 2000;107:1460–70.
2. Nygaard I, Barber MD, Burgio KL, et al. Prevalence of symptomatic pelvic floor disorders in US women. JAMA 2008;300:1311–6.
3. Samuelsson EC, Victor FT, Tibblin G, Svardsudd KF. Signs of genital prolapse in a Swedish population of women 20 to 59 years of age and possible related factors. Am J Obstet Gynecol 1999;180:299–305.
4. Luber KM, Boero S, Choe JY. The demographics of pelvic floor disorders: current observations and future projections. Am J Obstet Gynecol 2001;184:1496–501; discussion 1501-3.
5. Wu JM, Hundley AF, Fulton RG, Myers ER. Forecasting the prevalence of pelvic floor disorders in US women: 2010 to 2050. Obstet Gynecol 2009;114:1278–83.
6. Wu JM, Kawasaki A, Hundley AF, Dieter AA, Myers ER, Sung VW. Predicting the number of women who will undergo incontinence and prolapse surgery, 2010 to 2050. Am J Obstet Gynecol 2011;205:230.e1–5.
7. Siff LN, Barber MD. Native tissue prolapse repairs: comparative effectiveness trials. Obstet Gynecol Clin North Am 2016;43:69–81.
8. Olsen AL, Smith VJ, Bergstrom JO, Colling JC, Clark AL. Epidemiology of surgically managed pelvic organ prolapse and urinary incontinence. Obstet Gynecol 1997;89:501–6.

**9.** Jelovsek JE, Barber MD, Brubaker L, et al. Effect of uterosacral ligament suspension vs sacrospinous ligament fixation with or without perioperative behavioral therapy for pelvic organ vaginal prolapse on surgical outcomes and prolapse symptoms at 5 years in the OPTIMAL randomized clinical trial. JAMA 2018;319:1554–65.
**10.** Maher C, Feiner B, Baessler K, Schmid C. Surgical management of pelvic organ prolapse in women. Cochrane Database Syst Rev 2013:CD004014.
**11.** Milani R, Salvatore S, Soligo M, Pifarotti P, Meschia M, Cortese M. Functional and anatomical outcome of anterior and posterior vaginal prolapse repair with prolene mesh. BJOG 2005;112:107–11.
**12.** Lamblin G, Van-Nieuwenhuyse A, Chabert P, Lebail-Carval K, Moret S, Mellier G. A randomized controlled trial comparing anatomical and functional outcome between vaginal colposuspension and transvaginal mesh. Int Urogynecol J 2014;25:961–70.
**13.** Liang R, Abramowitch S, Knight K, et al. Vaginal degeneration following implantation of synthetic mesh with increased stiffness. BJOG 2013;120:233–43.
**14.** Feola A, Abramowitch S, Jallah Z, et al. Deterioration in biomechanical properties of the vagina following implantation of a high-stiffness prolapse mesh. BJOG 2013;120:224–32.
**15.** Feola A, Barone W, Moalli P, Abramowitch S. Characterizing the ex vivo textile and structural properties of synthetic prolapse mesh products. Int Urogynecol J 2013;24:559–64.
**16.** Shepherd JP, Feola AJ, Abramowitch SD, Moalli PA. Uniaxial biomechanical properties of seven different vaginally implanted meshes for pelvic organ prolapse. Int Urogynecol J 2012;23:613–20.
**17.** Gamble JG, Edwards CC, Max SR. Enzymatic adaptation in ligaments during immobilization. Am J Sports Med 1984;12:221–8.
**18.** Majima T, Yasuda K, Tsuchida T, et al. Stress shielding of patellar tendon: effect on small-diameter collagen fibrils in a rabbit model. J Orthop Sci 2003;8:836–41.
**19.** Woo SL, Gomez MA, Woo YK, Akeson WH. Mechanical properties of tendons and ligaments. II. The relationships of immobilization and exercise on tissue remodeling. Biorheology 1982;19:397–408.
**20.** Yamamoto N, Ohno K, Hayashi K, Kuriyama H, Yasuda K, Kaneda K. Effects of stress shielding on the mechanical properties of rabbit patellar tendon. J Biomech Eng 1993;115:23–8.
**21.** Badylak SF, Freytes DO, Gilbert TW. Reprint of: Extracellular matrix as a biological scaffold material: Structure and function. Acta Biomater 2015;23(Suppl):S17–26.
**22.** Brown BN, Ratner BD, Goodman SB, Amar S, Badylak SF. Macrophage polarization: an opportunity for improved outcomes in biomaterials and regenerative medicine. Biomaterials 2012;33:3792–802.
**23.** Nagatomi J, Toosi KK, Grashow JS, Chancellor MB, Sacks MS. Quantification of bladder smooth muscle orientation in normal and spinal cord injured rats. Ann Biomed Eng 2005;33:1078–89.
**24.** Liang R, Knight K, Barone W, et al. Extracellular matrix regenerative graft attenuates the negative impact of polypropylene prolapse mesh on vagina in rhesus macaque. Am J Obstet Gynecol 2017;216:153.e1–9.
**25.** Lowalekar SK, Cristofaro V, Radisavljevic ZM, Yalla SV, Sullivan MP. Loss of bladder smooth muscle caveolae in the aging bladder. Neurourol Urodyn 2012;31:586–92.
**26.** Song KS, Scherer PE, Tang Z, et al. Expression of caveolin-3 in skeletal, cardiac, and smooth muscle cells. Caveolin-3 is a component of the sarcolemma and co-fractionates with dystrophin and dystrophin-associated glycoproteins. J Biol Chem 1996;271:15160–5.
**27.** Liang R, Zong W, Palcsey S, Abramowitch S, Moalli PA. Impact of prolapse meshes on the metabolism of vaginal extracellular matrix in rhesus macaque. Am J Obstet Gynecol 2015;212:174.e1–7.
**28.** Skoczylas LC, Jallah Z, Sugino Y, et al. Regional differences in rat vaginal smooth muscle contractility and morphology. Reprod Sci 2013;20:382–90.
**29.** Jallah Z, Liang R, Feola A, et al. The impact of prolapse mesh on vaginal smooth muscle structure and function. BJOG 2016;123:1076–85.
**30.** Kramer J, Quensel C, Meding J, Cardoso MC, Leonhardt H. Identification and characterization of novel smoothelin isoforms in vascular smooth muscle. J Vasc Res 2001;38:120–32.
**31.** Barone WR, Moalli PA, Abramowitch SD. Textile properties of synthetic prolapse mesh in response to uniaxial loading. Am J Obstet Gynecol 2016;215:326.e1–9.
**32.** Otto J, Kaldenhoff E, Kirschner-Hermanns R, Muhl T, Klinge U. Elongation of textile pelvic floor implants under load is related to complete loss of effective porosity, thereby favoring incorporation in scar plates. J Biomed Mater Res A 2014;102:1079–84.
**33.** Bono N, Pezzoli D, Levesque L, et al. Unraveling the role of mechanical stimulation on smooth muscle cells: a comparative study between 2D and 3D models. Biotechnol Bioeng 2016;113:2254–63.
**34.** Shkumatov A, Thompson M, Choi KM, et al. Matrix stiffness-modulated proliferation and secretory function of the airway smooth muscle cells. Am J Physiol Lung Cell Mol Physiol 2015;308:L1125–35.
**35.** Grootaert MOJ, Moulis M, Roth L, et al. Vascular smooth muscle cell death, autophagy and senescence in atherosclerosis. Cardiovasc Res 2018;114:622–34.
**36.** Shea-Donohue T, Notari L, Sun R, Zhao A. Mechanisms of smooth muscle responses to inflammation. Neurogastroenterol Motil 2012;24:802–11.
**37.** Geng YJ, Wu Q, Muszynski M, Hansson GK, Libby P. Apoptosis of vascular smooth muscle cells induced by in vitro stimulation with interferon-gamma, tumor necrosis factor-alpha, and interleukin-1 beta. Arterioscler Thromb Vasc Biol 1996;16:19–27.
**38.** Boreham MK, Wai CY, Miller RT, Schaffer JI, Word RA. Morphometric analysis of smooth muscle in the anterior vaginal wall of women with pelvic organ prolapse. Am J Obstet Gynecol 2002;187:56–63.
**39.** Boreham MK, Wai CY, Miller RT, Schaffer JI, Word RA. Morphometric properties of the posterior vaginal wall in women with pelvic organ prolapse. Am J Obstet Gynecol 2002;187:1501–8; discussion 1508-9.
**40.** Northington GM, Basha M, Arya LA, Wein AJ, Chacko S. Contractile response of human anterior vaginal muscularis in women with and without pelvic organ prolapse. Reprod Sci 2011;18:296–303.
**41.** Liang R, Fawcett M, Shaffer R, Palcsey S, Moalli P. Impact of aging on vaginal smooth muscle: a morphometric study. Female Pelvic Med Reconstr Surg 2014;20(Suppl 4):S128.
**42.** Badylak SF, Gilbert TW. Immune response to biologic scaffold materials. Semin Immunol 2008;20:109–16.
**43.** Brown BN, Londono R, Tottey S, et al. Macrophage phenotype as a predictor of constructive remodeling following the implantation of biologically derived surgical mesh materials. Acta Biomater 2012;8:978–87.

## Author and article information

From the Department of Obstetrics and Gynecology, Larner College of Medicine at the University of Vermont, Burlington, VT (Dr Shaffer); the Department of Obstetrics, Gynecology, and Reproductive Sciences, Magee-Womens Research Institute, University of Pittsburgh, Pittsburgh, PA (Drs Liang, Knight, Carter-Brooks, and Moalli); and the Department of Bioengineering, University of Pittsburgh, Pittsburgh, PA (Dr Abramowitch).

[1]These authors contributed equally to this article.

Received Jan. 28, 2019; revised May 2, 2019; accepted May 10, 2019.

The views expressed herein are those of the authors and do not necessarily represent the official views of the National Institutes of Health. The funding source did not have involvement in the study design, data collection, analysis and interpretation, manuscript preparation, and the decision to submit the article for publication.

This study was supported by the National Institutes of Health grant R01 HD061811-01.

The authors report no conflict of interest.

Presented at the annual meetings of the American Urogynecologic Society, 2014 (Washington, DC), and 2017 (Providence, RI).

Corresponding author: Pamela M. Moalli, MD, PhD. pmoalli@mail.magee.edu